Dalton Transactions

Accepted Manuscript

ROYAL SOCIETY OF CHEMISTRY

www.rsc.org/dalton

Journal Name

ARTICLE

Insights into the dehydrogenation reaction process of a K-containing $Mg(NH_2)_2$-2LiH system

Received 00th January 20xx,
Accepted 00th January 20xx

DOI: 10.1039/x0xx00000x

www.rsc.org/

Yongfeng Liu,[a,b] Yaxiong Yang[a], Xin Zhang,[a] You Li,[a] Mingxia Gao[a] and Hongge Pan[a,*]

The thermal dehydrogenation process of the KOH-containing $Mg(NH_2)_2$-2LiH system was systematically investigated by identifying changes in the structure and composition of its components by XRD and FTIR. During ball milling, the added KOH reacts with $Mg(NH_2)_2$ and LiH to produce MgO, KH and $Li_2K(NH_2)_3$. During the initial heating process (<120 °C), the newly formed KH and $Li_2K(NH_2)_3$ react with $Mg(NH_2)_2$ and LiH to yield MgNH, $LiNH_2$ and $Li_3K(NH_2)_4$ along with a hydrogen release. Raising the temperature to 185 °C results in a reaction between $Mg(NH_2)_2$, MgNH and LiH that gives $Li_2Mg_2N_3H_3$ as the product and further releases hydrogen. As the temperature is increased to 220 °C, $Li_2Mg_2N_3H_3$ reacts with $LiNH_2$ and LiH to produce $Li_2MgN_2H_2$ and H_2. Meanwhile, two parallel reactions between $Li_2Mg_2N_3H_3$, $Li_3K(NH_2)_4$ and LiH also generate additional hydrogen. Specifically, the KH and $Li_2K(NH_2)_3$, formed *in situ* during ball milling, serve as reactants in the dehydrogenation reaction of the $Mg(NH_2)_2$-2LiH system, which is responsible for the significantly improved thermodynamics and kinetics of hydrogen storage.

Introduction

With an ever-increasing demand for safe, efficient and economical hydrogen storage, a growing number of research interests have included complex hydrides, including metal alanates, borohydrides, and amides; ammonia borane; and amidoboranes.[1-7] Among these complexes, metal amide/hydride combination systems are regarded as one of the most promising candidates due to their high hydrogen capacities, flexible compositions and variable thermodynamics and kinetics.[8-9] In 2002, Chen et al. reported for the first time that lithium nitride (Li_3N) could reversibly store 11.4 wt% of hydrogen at elevated temperatures, and the resultant product was a $LiNH_2$-2LiH mixture.[10] Following this work, a variety of metal amide/hydride combinations have been explored and studied for their hydrogen storage properties.[11-19] In particular, the $Mg(NH_2)_2$-2LiH system exhibits moderate operating temperatures, appropriate thermodynamics, good reversibility, and a relatively high hydrogen capacity of 5.6 wt% and has therefore attracted considerable attention.[11-12] More importantly, the thermodynamically predicated operating temperature is approximately 90 °C at 1 bar, which are close to the practical conditions for proton exchange membrane fuel cells (PEMFCs) that have been proposed by US Department of Energy (DOE).[20,21] However, sufficient hydrogen desorption has only been achieved at temperatures of up to 250 °C, which is due to the high kinetic barrier.[11-12]

For hydrogen storage in the $Mg(NH_2)_2$-2LiH system, there have been numerous efforts devoted to reducing the operating temperature and improving the reaction kinetics by introducing additives or catalysts, such as $Li_2MgN_2H_2$, carbon nanotubes, transition metals and their compounds, metal borohydrides, alkali-metal compounds, and so forth.[22-40] Among these known additives and catalysts, alkali-metal compounds have exhibited superior catalytic activities.[31-40] Liu et al. have reported that partially substituting Mg or Li in $Mg(NH_2)_2$-2LiH with Na reduced the dehydrogenation temperature by 10 °C. The majority of hydrogen desorption in the $Mg(NH_2)_2$-2LiH-0.5NaOH system was complete at a temperature below 175 °C, more than a 30 °C reduction in comparison with the pristine sample.[31] In 2009, Wang et al. disclosed that introducing a small amount of KH induced a significant shift in the dehydrogenation peak temperature from 186 °C to 132 °C.[32] More encouragingly, reversible hydrogen storage could even proceed at a temperature as low as 107 °C in a pressure-composition-temperature (PCT) model. Such an improvement has stimulated intense interest, and investigations have expanded to other K-, Rb- and Cs-based compounds.[33-40] Recently, we have revealed the effects of potassium halides and demonstrated that a sample with 0.08 KF added to $Mg(NH_2)_2$-2LiH could reversibly store 5.0 wt% hydrogen with an onset dehydrogenation temperature of 80 °C.[34] Additionally, a hydrogen release from $Mg(NH_2)_2$-2LiH-

[a]*State Key Laboratory of Silicon Materials, Key Laboratory of Advanced Materials and Applications for Batteries of Zhejiang Province and School of Materials Science and Engineering, Zhejiang University, Hangzhou 310027, China. Fax: +86 571 87952615, E-mail: hgpan@zju.edu.cn*
[b]*Key Laboratory of Advanced Energy Materials Chemistry (Ministry of Education), Nankai University, Tianjin 300071, China*
†Electronic Supplementary Information (ESI) available: FTIR and XRD of $Li_2Mg_2N_3H_3$ and dehydrogenated $Mg(NH_2)_2$-2LiH-0.07KOH; FTIR spectra of $Li_3K(NH_2)_4$ and dehydrogenated $Mg(NH_2)_2$-2LiH-0.2KOH. See DOI: 10.1039/x0xx00000x

0.07KOH had been observed to begin at ~ 75 °C and peak at 120 °C,[35] which is superior to even the KH-containing sample. It has been found that during ball milling the KOH reacts with $Mg(NH_2)_2$ and LiH to form MgO, KH and $Li_2K(NH_2)_3$, which work together to improve the thermodynamics and kinetics of hydrogen storage. Unfortunately, the detailed dehydrogenation reaction process of the KOH-added $Mg(NH_2)_2$-2LiH system remains unclear.

In this work, the dehydrogenation reaction mechanism of the $Mg(NH_2)_2$-2LiH-0.07KOH system was systematically studied by characterizing the changes in composition and structure at different stages of the hydrogenation/dehydrogenation process. It was determined that upon both dynamic heating and isothermal dehydrogenation, KH and $Li_2K(NH_2)_3$, which is formed during ball milling, took part in the dehydrogenation reaction of the $Mg(NH_2)_2$-2LiH system as reactants and should be the most important factor behind the significantly improved hydrogen storage thermodynamics and kinetics.

Experimental section

Commercial chemicals LiH (98%) and KOH (95%) were purchased from Alfa Aesar and Aladdin, respectively, and used as received. $Mg(NH_2)_2$ was synthesized in our laboratory by reacting Mg powder (Sinopharm, 99%) with ammonia at 7.0 bar and 300 ºC. The $Mg(NH_2)_2$-2LiH-0.07KOH sample was prepared by ball milling the corresponding mixture under 80 bar H_2 in a planetary ball mill (QM-3SP4, Nanjing). A homemade Temperature-Programmed-Desorption (TPD) system that was attached to an online mass spectrometer (MS) and a PCTPRO-2000 Sievert-type pressure-composition-temperature (PCT) apparatus were used to determine the dehydrogenation behaviours. In a TPD experiment, approximately 50 mg of sample was loaded and tested each time using pure Ar as the carrier gas, and the temperature was elevated at a rate of 2 °C/min. For a PCT measurement, approximately 500 mg of sample was used and the operating temperature was set at 140 °C.

The phase structures of samples were identified by means of powder X-ray diffraction (XRD) using a PANalytical X'Pert diffractometer equipped with Cu Kα radiation (40 KV and 40 mA). Data were collected from 10° to 90° (2ϑ) with step increments of 0.05° at ambient temperature. A homemade container was employed to prevent water and oxygen contamination during sample transfer and scanning. Fourier transform infrared (FTIR) spectra were recorded on a Bruker Tensor 27 Fourier Transform Infrared Spectroscopy with a resolution of 4 cm^{-1}. An air tight container was used to prevent the powder sample from air and moisture contamination during the measurements. Approximately 10 mg of powder was loaded into the air tight container in a glovebox that was filled with purified argon. Reflection mode was used and each FTIR spectrum was created from an average of 32 scans.

Results and discussion

The $Mg(NH_2)_2$-2LiH-0.07KOH sample was prepared by ball milling the corresponding mixture under 80 bar H_2 in a planetary ball mill. To investigate the chemical processes that occurred during thermal dehydrogenation, samples at different stages of the dehydrogenation processes were collected under non-equilibrium (TPD model) and equilibrium (PCT model) conditions for the FTIR and XRD analyses. Fig. 1(a) shows the typical TPD curve of the $Mg(NH_2)_2$-2LiH-0.07KOH sample. Hydrogen desorption started at ~ 75 °C and terminated at 220 °C and was associated with a main peak at 155 °C and a shoulder at 120 °C. This is in excellent agreement with our previous report.[35] As shown in the TPD curve, five samples were collected as non-equilibrium dehydrogenation products at 100, 120, 160, 185 and 220 °C. Fig. 1(b) provides the plot for the $Mg(NH_2)_2$-2LiH-0.07KOH sample at 140 °C, which demonstrates a typical PCT desorption curve. A plateau in H content is observed from 4.9 to 1.8 wt%, and a sloping region is noted for H content from 1.8 wt% to 0 wt%. As is also shown in Fig. 1(b), five additional samples were collected at hydrogen release of 0.55, 0.9, 2.1, 3.1 and 4.9 wt% as equilibrium dehydrogenation products.

Fig. 2 presents the FTIR spectra of the $Mg(NH_2)_2$-2LiH-0.07KOH system as a function of temperature, i.e., at different non-equilibrium dehydrogenation stages. The characteristic N-H vibrations of $Mg(NH_2)_2$ at 3327 and 3272 cm^{-1} were readily apparent in the FTIR spectrum of the sample dehydrogenated at 100 °C. A weak absorption peak centred at ~ 3193 cm^{-1} was also noted and can be assigned to the N-H stretch of poorly crystallized MgNH, as reported previously.[19,41] While the dehydrogenation temperature was elevated to 120 °C, this absorbance at 3193 cm^{-1} intensified, but the relative intensities of the $Mg(NH_2)_2$ peaks decreased, which suggests the consumption of $Mg(NH_2)_2$ at elevated temperatures. Further increasing the dehydrogenation temperature to 160 °C resulted in the detection of the typical absorption peaks assigned to $LiNH_2$ at 3312 and 3257 cm^{-1}, along with an absence of the absorption peaks of $Mg(NH_2)_2$ at 3327 and 3272 cm^{-1}. In particular, the N-H absorption belonging to the imide

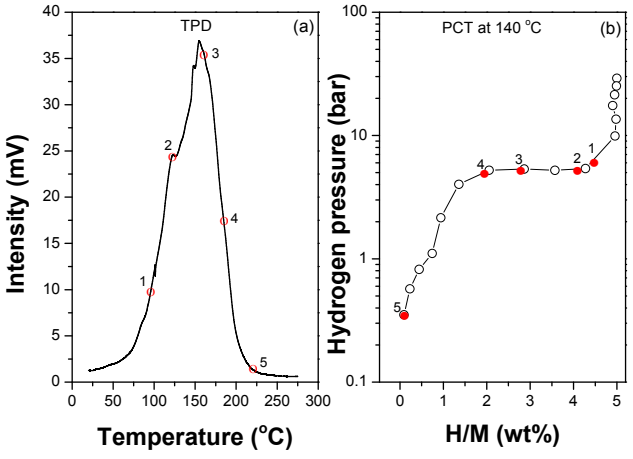

Fig. 1 TPD (a) and PCT (b) curves of the $Mg(NH_2)_2$-2LiH-0.07KOH sample.

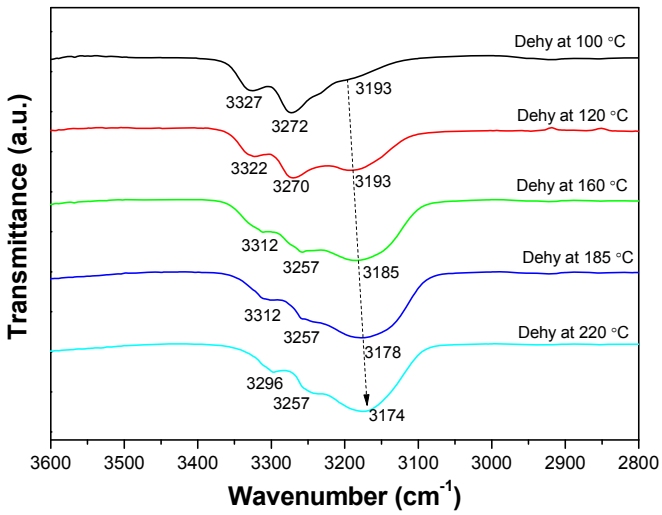

Fig. 2 FTIR spectra of the dehydrogenated $Mg(NH_2)_2$-2LiH-0.07KOH system as a function of temperature.

shifted to a lower wavenumber (3185 cm^{-1}), which is in good agreement with the spectrum of $Li_2Mg_2N_3H_3$ (Fig. S1, ESI†). These results indicate that at 120–160 °C, $Mg(NH_2)_2$ and MgNH were consumed by reacting with LiH to give rise to the formation of $LiNH_2$ and $Li_2Mg_2N_3H_3$. As the temperature was elevated to 185 °C, the N-H absorbance of the imide further shifted to 3178 cm^{-1} and the peaks attributed to $LiNH_2$ at 3312 and 3257 cm^{-1} were weakened, which reveals that $LiNH_2$ was consumed with the release of more hydrogen. After dehydrogenation stopped at 220 °C, the absorption peak centred at 3174 cm^{-1} dominated the FTIR spectrum and is assigned to the cubic $Li_2MgN_2H_2$ phase, according to the literatures.[28,42] Moreover, two weak and broad absorption peaks centred at 3296 and 3257 cm^{-1}, which are ascribed to $Li_3K(NH_2)_4$, were also observed in the FTIR spectrum.

Fig. 3 presents the XRD patterns of the $Mg(NH_2)_2$-2LiH-0.07KOH system as a function of temperature. As shown in Fig. 3, the characteristic peaks of $Mg(NH_2)_2$ and LiH were clearly observed in the XRD pattern of the sample dehydrogenated at 100 °C, along with two new diffraction peaks at 30.1° and 51.1°. Between 100 °C and 120 °C, these two newly developed peaks intensified, whereas the diffraction peaks of $Mg(NH_2)_2$ and LiH weakened. To identify the phase with diffraction peaks at 30.1° and 51.1°, a newly designed sample, which released a quantity of hydrogen in PCT mode that was identical to the amount released during TPD, was prepared and collected for FTIR and XRD analyses. The results are shown in Fig. 4. After releasing 0.55 wt% H_2 under conditions of equilibrium, six phases were distinctly detected by means of XRD and FTIR: $LiNH_2$, MgNH, KH, MgO, LiH and $Mg(NH_2)_2$. It is therefore believed that the diffraction peaks at 30.1° and 51.1°, shown in Fig. 3, likely belong to $LiNH_2$. However, it is strange that no K-containing phase was detected below 120 °C by means of XRD and FTIR. To identify the status of potassium, an additional FTIR spectrum was acquired on the $Mg(NH_2)_2$-2LiH-0.2KOH sample that was dehydrogenated at 100 °C. In addition to the typical doublet N-H vibration of $LiNH_2$ at 3258 and 3312 cm^{-1} and the single peak belonging to MgNH at 3193 cm^{-1}, an asymmetric shoulder at 3297 cm^{-1} was also observed although its intensity was rather weak. It is possible that this feature originates from a new lithium potassium amide $Li_3K(NH_2)_4$ (Fig. S2, ESI†). Recent investigations have also revealed that KNH_2 could react with $LiNH_2$ to form $Li_3K(NH_2)_4$ at a low temperature of 100 °C.[43] We therefore deduce that $Li_2K(NH_2)_3$ and KH formed during ball milling and then reacted with LiH and $Mg(NH_2)_2$ to generate $Li_3K(NH_2)_4$ and MgNH upon heating. However, the low concentration, as well as a peak position adjacent to $Mg(NH_2)_2$ and $LiNH_2$, make detection of the $Li_3K(NH_2)_4$ phase in the $Mg(NH_2)_2$-2LiH-0.07KOH sample with XRD and FTIR difficult.

Further elevating the dehydrogenation temperature to 160 °C resulted in a weakening of the typical diffraction peaks associated with $Mg(NH_2)_2$ and LiH, while those of $Mg(NH_2)_2$ disappeared (Fig. 3), which represents the complete consumption of $Mg(NH_2)_2$. However, the newly developed diffraction peaks at 30.1° and 51.1° were further intensified and accompanied by a slight high-angle shift, in addition to the emergence of a peak at 60.6°, which probably correspond to the $LiNH_2$ and $Li_2Mg_2N_3H_3$ phases that were observed by FTIR (Fig. 2). After dehydrogenation at 185 °C, a broad diffraction peak was observed in the 2ϑ range of 12.8–22.4°, which may originate from the overlapping diffraction peaks of $LiNH_2$, $Li_2Mg_2N_3H_3$ and $Li_2MgN_2H_2$, because they all appear in this region.[44] For the sample dehydrogenated at 220 °C, the diffraction peaks assigned to the cubic $Li_2MgN_2H_2$ phase were presented in the XRD pattern.

On the basis of the above discussion, we attempt to picture the chemical process during thermal dehydrogenation of the post-milled $Mg(NH_2)_2$-2LiH-0.07KOH system. As has been reported previously,[35] the added KOH reacted with $Mg(NH_2)_2$ and LiH to give rise to the formation of MgO, KH and $Li_2K(NH_2)_3$. As a consequence of this, the $Mg(NH_2)_2$-2LiH-0.07KOH system converted to a more complicated composite with the composition 1.93$Mg(NH_2)_2$-1.907LiH-0.023KH-0.047$Li_2K(NH_2)_3$-0.07MgO.

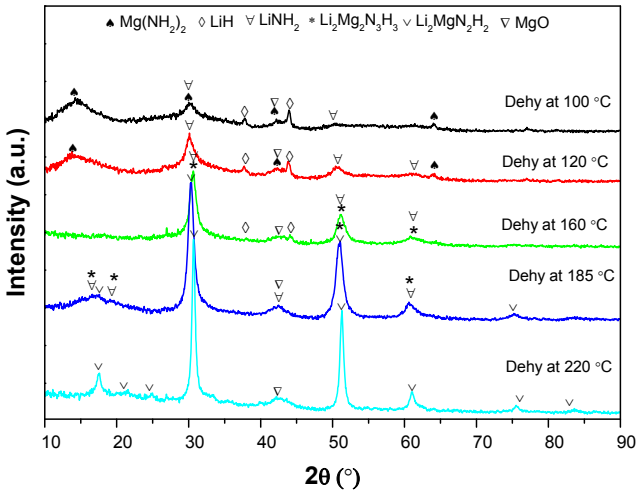

Fig. 3 XRD patterns of the dehydrogenated $Mg(NH_2)_2$-2LiH-0.07KOH system as a function of temperature.

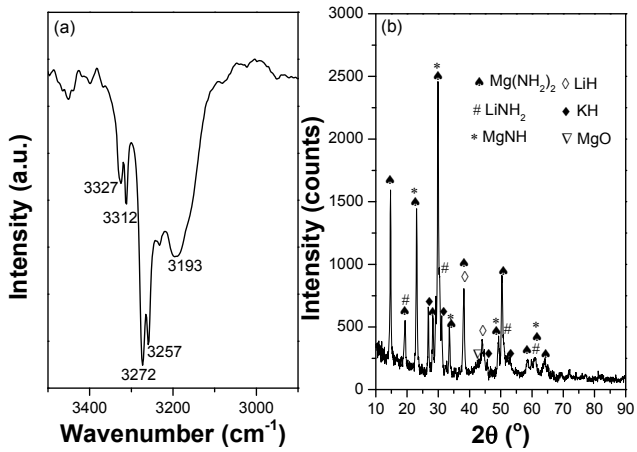

Fig. 4 FTIR spectrum (a) and XRD pattern (b) of the $Mg(NH_2)_2$-2LiH-0.07KOH system with a 0.55 wt% hydrogen release..

$$Mg(NH_2)_2+\frac{4}{3}LiH+KOH \rightarrow \frac{2}{3}Li_2K(NH_2)_3+MgO+\frac{1}{3}KH+H_2 \quad (1)$$

During the initial heating process (<120 °C), the reaction between KH, $Li_2K(NH_2)_3$, $Mg(NH_2)_2$ and LiH first yielded MgNH, $LiNH_2$ and $Li_3K(NH_2)_4$, along with a hydrogen release.

$$KH+2Li_2K(NH_2)_3+20Mg(NH_2)_2+19LiH \longrightarrow 20MgNH+14LiNH_2+3Li_3K(NH_2)_4+20H_2 \quad (2)$$

Further raising the operating temperature to 185 °C produced $Li_2Mg_2N_3H_3$, depleted MgNH and $Mg(NH_2)_2$, and decreased the amount of LiH.

$$Mg(NH_2)_2+MgNH+2LiH \rightarrow Li_2Mg_2N_3H_3+2H_2 \quad (3)$$

As the temperature was increased to 220 °C, $Li_2MgN_2H_2$ was detected as the resultant product, whereas $LiNH_2$, LiH and the previously produced $Li_2Mg_2N_3H_3$ were consumed.

$$Li_2Mg_2N_3H_3+LiNH_2+LiH \rightarrow 2Li_2MgN_2H_2+H_2 \quad (4)$$

In the present study, ~ 0.023 mol KH and 0.047 mol $Li_2K(NH_2)_3$ were formed after ball milling the mixture of $Mg(NH_2)_2$-2LiH-0.07KOH, as mentioned above. Therefore, the theoretical hydrogen release from reactions (2)-(4) were calculated to be approximately 1.23, 2.43, and 0.86 wt% versus the post-milled $Mg(NH_2)_2$-2LiH-0.07KOH system. In total, only 4.52 wt% of hydrogen is released from the abovementioned reactions, which is clearly lower than the experimental result (4.92 wt%) that has been previously reported.[35] Therefore, we speculate that an additional reaction took place between 185–220 °C. Further analyses revealed that the ~ 0.134 mol $Li_2Mg_2N_3H_3$ and 0.218 mol LiH first thought to be produced during reactions (2)–(4) were overestimated. Thus, it is believed that the additional hydrogen originated from the chemical reaction between $Li_2Mg_2N_3H_3$ and LiH.

$$2Li_2Mg_2N_3H_3+2LiH \rightarrow Li_2MgN_2H_2+2Li_2NH+Mg_3N_2+2H_2 \quad (5)$$

Theoretically, ~ 0.35 wt% of hydrogen (versus the post-milled $Mg(NH_2)_2$-2LiH-0.07KOH) can be evolved from reaction (5), which is provided by reacting 0.134 mol $Li_2Mg_2N_3H_3$ with 0.134 mol LiH. Such a reaction was directly verified by preparing the $Li_2Mg_2N_3H_3$-LiH mixture (Fig. 5). Moreover, the presence of $Li_3K(NH_2)_4$ and MgO dramatically decreases the dehydrogenation temperature of the $Li_2Mg_2N_3H_3$-LiH mixture. However, it should be noted that the newly designed $0.134Li_2Mg_2N_3H_3$-0.218LiH-$0.07Li_3K(NH_2)_4$-0.07MgO sample liberates ~ 0.52 wt% of hydrogen (versus the post-milled $Mg(NH_2)_2$-2LiH-0.07KOH), which is higher than the theoretical hydrogen capacity of reaction (5). We therefore deduce that at this temperature the chemical reaction between a portion of $Li_3K(NH_2)_4$ and an excess of LiH may further proceed to release more hydrogen. As shown in Fig. 6, the 0.084LiH-$0.07Li_3K(NH_2)_4$-0.07MgO sample released ~ 0.21 wt% of hydrogen (versus the post-milled $Mg(NH_2)_2$-2LiH-0.07KOH) to form the resultant product of a new imide-amide complex with the chemical formula $Li_6K(NH)_3(NH_2)$. A similar mixed imide-amide complex of $KMg(NH)(NH_2)$ in the $Mg(NH_2)_2$-KH system was also observed by Wang et al.[45]

$$3LiH+Li_3K(NH_2)_4 \rightarrow Li_6K(NH)_3(NH_2)+3H_2 \quad (6)$$

Thus, 0.084 mol LiH can react with 0.028 mol $Li_3K(NH_2)_4$ to release a theoretical maximum of 0.22 wt% of hydrogen, which results in residual $Li_3K(NH_2)_4$ in the final product after full dehydrogenation (Fig. 6). Moreover, it should be noted that the rapid hydrogen desorption from the 0.084LiH-$0.07Li_3K(NH_2)_4$-0.07MgO sample only occurs above 185 °C, implying that $Li_3K(NH_2)_4$ may remain essentially unchanged in the temperature range of 120–185 °C. Taking into account reactions (1)–(6), a total dehydrogenation capacity of 5.09 wt% was achieved for the post-milled $Mg(NH_2)_2$-2LiH-0.07KOH sample, which is in excellent agreement with a previous experimental result.[35] Here, it should be pointed out that the low concentration, and/or the structural similarity of Li_2NH, Mg_3N_2 and $Li_6K(NH)_3(NH_2)$ with $Li_2MgN_2H_2$ are responsible for

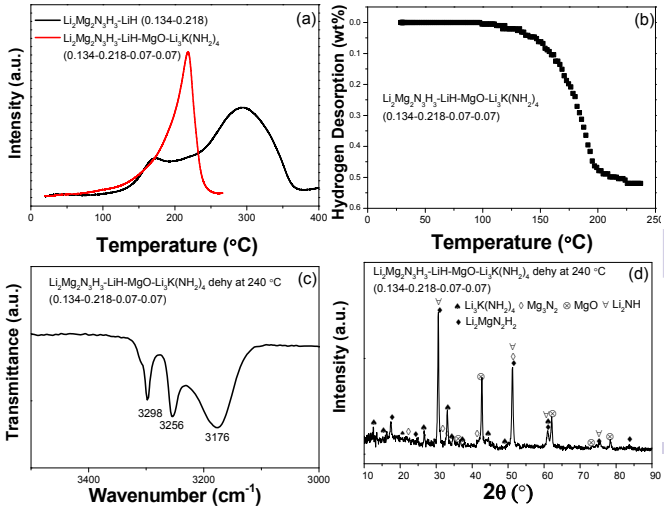

Fig. 5 TPD (a) and volumetric release (b) curves of the designed $Li_2Mg_2N_3H_3$-LiH system and the FTIR spectrum (c) and XRD pattern (d) of the sample after dehydrogenation.

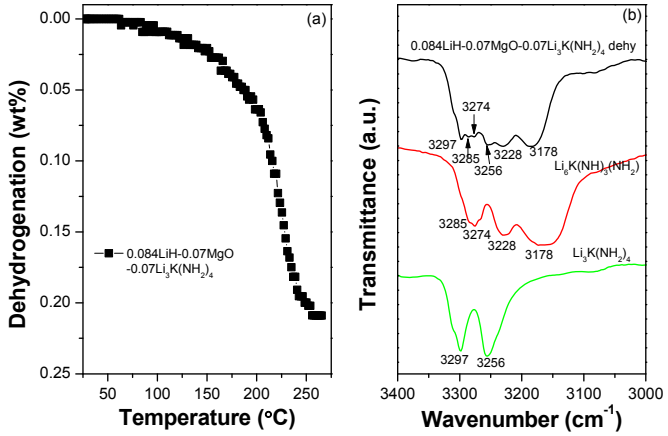

Fig. 6 Volumetric release curve (a) of the designed $Li_3K(NH_2)_4$-LiH system and the FTIR spectrum (b) of the sample after dehydrogenation.

the inability to detect the latter compound by XRD and FTIR during dehydrogenation of the $Mg(NH_2)_2$-2LiH-0.07KOH system, as shown in Fig. 2 and 3.

To verify reactions (3)-(6), a new mixture with the composition of $0.47Mg(NH_2)_2$-$1.471LiH$-$0.46MgNH$-$0.322LiNH_2$-$0.07Li_3K(NH_2)_4$-$0.07MgO$, which corresponds to the first-step dehydrogenation product, was designed and prepared. It was observed that the sample prepared by low-energy ball milling exhibited a very similar dehydrogenation behaviour to the second-stage dehydrogenation that was observed at increased temperatures, as shown in Fig. 7. This provides strong evidence for reaction (2). Moreover, the fact that only one major peak was observed for the second-stage dehydrogenation in the TPD curve reveals that reactions (3)–(6) likely possess very similar kinetics, as mentioned above.

Further FTIR and XRD analyses on the dehydrogenated $Mg(NH_2)_2$-2LiH-0.07KOH system under equilibrium conditions were conducted to confirm the above structural change, as shown in Figs. 4 and 8. It was found that the samples that released 0.55 and 0.9 wt% hydrogen primarily consisted of $Mg(NH_2)_2$, $LiNH_2$, MgNH, KH, LiH and MgO. After liberating 2.1

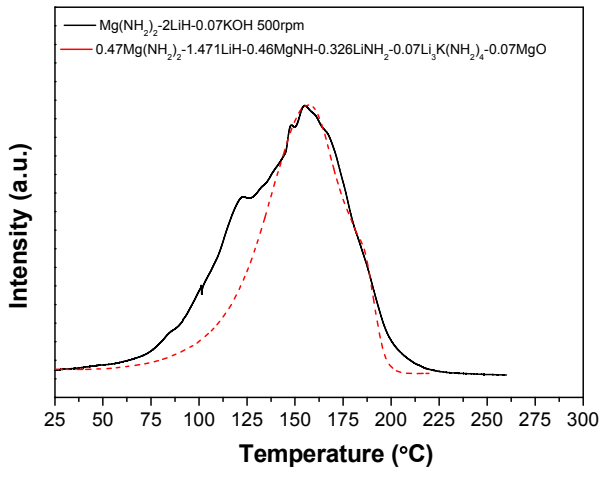

Fig. 7 Comparison of the TPD curves for the $Mg(NH_2)_2$-2LiH-0.07KOH and $0.47Mg(NH_2)_2$-$1.471LiH$-$0.46MgNH$-$0.322LiNH_2$-$0.07Li_3K(NH_2)_4$-$0.07MgO$ samples.

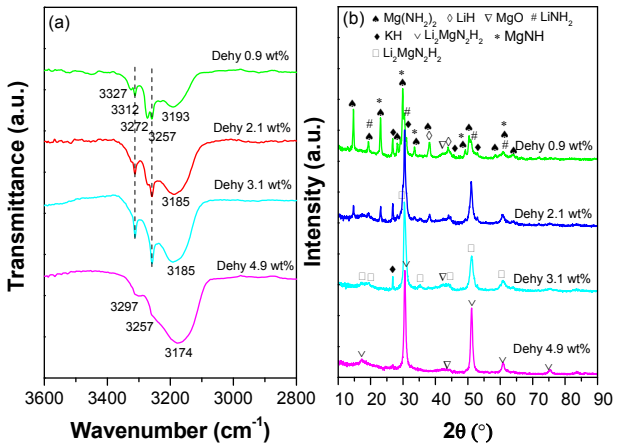

Fig. 8 FTIR spectra (a) and XRD patterns (b) of the dehydrogenated $Mg(NH_2)_2$-2LiH-0.07KOH system while at equilibrium.

and 3.1 wt% hydrogen, $Li_2Mg_2N_3H_3$ was detected, and $Mg(NH_2)_2$ and MgNH were absent (Fig. S3, ESI†). With a hydrogen release of 4.9 wt%, $Li_2MgN_2H_2$ and $Li_3K(NH_2)_4$ were the only phases identified by XRD and FTIR. At first glance, the dehydrogenation process resembles the non-equilibrium state. However, unlike the TPD experiment, it is interesting to note that KH was distinctly detected in the dehydrogenation process under equilibrium conditions and was gradually consumed by the release of hydrogen, which concurs with the results reported by Wang et al.[45] This is possibly because $Li_2K(NH_2)_3$ reacts with LiH in the presence of hydrogen to convert into $Li_3K(NH_2)_4$, $LiNH_2$ and KH.

$$2Li_2K(NH_2)_3+LiH \xrightarrow{H_2} Li_3K(NH_2)_4+2LiNH_2+KH \quad (7)$$

Such a reaction was proved by heating a mixture of $Li_2K(NH_2)_3$-LiH under 100 bar of hydrogen and at 140 °C, as shown in Fig. 9. Clearly, the hydrogenated $Li_2K(NH_2)_3$-LiH sample was mainly composed of $Li_3K(NH_2)_4$, $LiNH_2$ and KH. Additionally, after heating the $7LiNH_2$-KNH_2 mixture up to 300 °C in an ammonia atmosphere, the resultant product continued to consist of $Li_3K(NH_2)_4$ and $LiNH_2$, which further confirmed the good

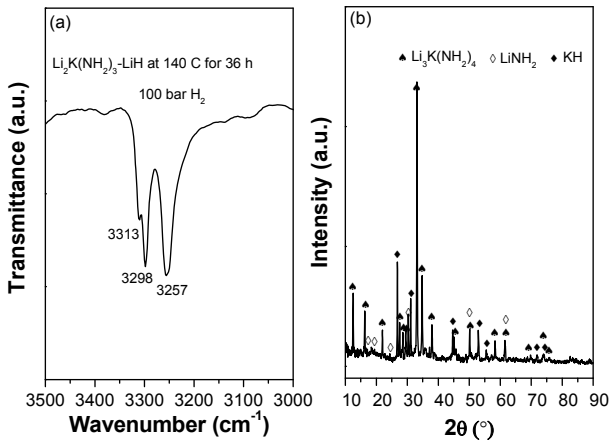

Fig. 9 FTIR spectrum (a) and XRD pattern (b) of the $Li_2K(NH_2)_3$-LiH sample after heating at 140 °C and with 100 bar of hydrogen.

thermodynamically stability of $Li_3K(NH_2)_4$. However, as the hydrogen pressure was lower than a specific value, it is likely that KH proceeded to react with $Li_2Mg_2N_3H_3$, $LiNH_2$ and LiH to yield $Li_3K(NH_2)_4$ and $Li_2MgN_2H_2$. Under equilibrium conditions, this process is responsible for the disappearance of KH and the generation of $Li_3K(NH_2)_4$ after complete dehydrogenation, as shown in Fig. 9. Consequently, we can deduce that hydrogen desorption from the post-milled $Mg(NH_2)_2$-2LiH-0.07KOH at equilibrium possibly underwent a slightly different reaction process with respect to the dynamic desorption. In addition, it is worth mentioning that Wang et al. have recently reported that KH could react with $Mg(NH_2)_2$ to yield $K_2Mg(NH_2)_4$, MgNH and hydrogen between 60–180 °C.[45] However, FTIR peaks that were associated with $K_2Mg(NH_2)_4$ at 3355, 3331, 3303, 3283, 3234, and 3225 cm^{-1} were not been detected in the $Mg(NH_2)_2$-2LiH-0.07KOH system in the present study, which may be due to the presence of $Li_2K(NH_2)_3$ and LiH, which could change the reaction pathways of the $Mg(NH_2)_2$-KH system.

Conclusions

In this study, the detailed dehydrogenation process of the KOH-containing $Mg(NH_2)_2$-2LiH system was investigated by characterizing the changes in the structure and composition at different stages of the process. Upon dynamic heating, the KH and $Li_2K(NH_2)_3$, which was formed *in situ* in the ball milling process, first reacted with $Mg(NH_2)_2$ and LiH to yield MgNH, $LiNH_2$ and $Li_3K(NH_2)_4$, along with the release of hydrogen (< 120 °C). Subsequently, the reaction between $Mg(NH_2)_2$, MgNH and LiH produced $Li_2Mg_2N_3H_3$ and a further release hydrogen (120–185 °C). Finally, $Li_2Mg_2N_3H_3$ reacted with $LiNH_2$ and LiH to form $Li_2MgN_2H_2$ and H_2 (185–220 °C). At the same time, a series of parallel reactions between $Li_2Mg_2N_3H_3$, $Li_3K(NH_2)_4$ and LiH proceeded to release additional hydrogen. Consequently, the reactivity of K-based compounds should be the most important factor behind the significantly improved thermodynamic and kinetic properties associated with hydrogen storage in the KOH-containing $Mg(NH_2)_2$-2LiH system. In an isothermal experiment, however, KH remained constant throughout the initial dehydrogenation stage (< 3.1 wt%) and was then converted to $Li_3K(NH_2)_4$ upon the further release of hydrogen. Thus, a slightly different reaction process occurred, with respect to the dynamic desorption, due to the presence of hydrogen in the reaction environment.

Acknowledgements

We gratefully acknowledge the financial support received from the National Natural Science Foundation of China (51171170, 51222101), the Research Fund for the Doctoral Program of Higher Education of China (20130101110080, 20130101130007), the Program for Innovative Research Team in the University of Ministry of Education of China (IRT13037), and the Fundamental Research Funds for the Central Universities (2014XZZX003-08, 2014XZZX005).

Notes and references

1 L. Schlapbach and A. Züttel, *Nature*, 2001, **414**, 353–358.
2 S. I. Orimo, Y. Nakamori, J. R. Eliseo, A. Züttel and C. M. Jensen, *Chem. Rev.*, 2007, **107**, 4111–4132.
3 I. P. Jain, P. Jain and A. Jain, *J. Alloys Compd.*, 2010, **503**, 303–339.
4 L. Li, C. C. Xu, C. C. Chen, Y. J. Wang, L. F. Jiao and H. T. Yuan, *Int. J. Hydrogen Energy*, 2013, **38**, 8798–8812.
5 Y. S. Chua, P. Chen, G. T. Wu and Z. T. Xiong, *Chem. Comm.*, 2011, **47**, 5116–5129.
6 H. W. Li, Y. G. Yan, S. Orimo, A. Züttel and C. M. Jensen, *Energies*, 2011, **4**, 185–214.
7 M. B. Ley, L. H. Jepsen, Y. S. Lee, Y. W. Cho, J. M. B. von Colbe, M. Dornheim, M. Rokni, J. O. Jensen, M. Sloth, Y. Filinchuk, J. E. Jørgensen, F. Besenbacher and T. R. Jensen, *Mater. Today*, 2014, **17**, 122–128.
8 C. Liang, Y. F. Liu, H. L. Fu, Y. F. Ding, M. X. Gao and H. G. Pan, *J. Alloys Compd.*, 2011, **509**, 7844–7853.
9 J. H. Wang, H. W. Li and P. Chen, *MRS Bull.*, 2013, **38**, 480–487.
10 P. Chen, Z. T. Xiong, J. Z. Luo, J. Y. Lin and K. L. Tan, *Nature*, 2002, **420**, 302–304.
11 Z. T. Xiong, G. T. Wu, H. J. Hu and P. Chen, *Adv. Mater.*, 2004, **16**, 1522–1525.
12 W. F. Luo, *J. Alloys Compd*., 2004, **381**, 284–287.
13 H. Y. Leng, T. Ichikawa, S. Hino, T. Nakagawa and H. Fujii, *J. Phys. Chem. B*, 2005, **109**, 10744–10748.
14 J. Lu, Z. Z. Fang and H. Y. Sohn, *J. Phys. Chem. B*, 2006, **110**, 14236–14239.
15 Y. F. Liu, K. Zhong, M. X. Gao, J. H. Wang, H. G. Pan and Q. D. Wang, *Chem. Mater.*, 2008, **20**, 3521–3527.
16 Z. T. Xiong, G. T. Wu, J. J. Hu, Y. F. Liu, P. Chen, W. F. Luo and J. Wang, *Adv. Funct. Mater.*, 2007, **17**, 1137–1142.
17 Y. F. Liu, F. H. Wang, Y. H. Cao, M. X. Gao and H. G. Pan, *Int. J. Hydrogen Energy*, 2010, **35**, 8343–8349.
18 J. J. Hu, E. Röhm and M. Fichtner, *Acta Mater.*, 2011, **59**, 5821–5831.
19 B. Paik, H. W. Li, J. H. Wang and E. Akiba, *Chem. Comm.*, 2015, **51**, 10018–10021.
20 Z. Xiong, J. Hu, G. Wu, P. Chen, W. Luo, K. Gross and J. Wang, *J. Alloys Compd.*, 2005, **398**, 235–239.
21 http://energy.gov/sites/prod/files/2015/05/f22/fcto_targets_onboard_hydro_storage_explanation.pdf.
22 A. Sudik, J. Yang, D. Halliday and C. Wolverton, *J. Phys. Chem. C*, 2007, **111**, 6568–6573.
23 Y. F. Liu, K. Zhong, K. Luo, M. X. Gao, H. G. Pan and Q. D. Wang, *J. Am. Chem. Soc.* 2009, **131**, 1862–1870.
24 Y. Chen, P. Wang, C. Liu and H. M. Cheng, *Int. J. Hydrogen Energy*, 2007, **32**, 1262–1268.
25 L. P. Ma, H. B. Dai, Y. Liang, X. D. Kang, Z. Z. Fang, P. J. Wang, P. Wang and H. M. Cheng, *J. Phys. Chem. C*, 2008, **112**, 18280–18285.
26 R. R. Shahi, T. P. Yadav, M. A. Shaz, and O. N. Srivastva, *Int. J. Hydrogen Energy*, 2010, **35**, 238–246.
27 J. J. Hu, Y. F. Liu, G. T. Wu, Z. T. Xiong, Y. S. Chua and P. Chen, *Chem. Mater.*, 2008, **20**, 4398–4402.
28 C. Liang, Y. F. Liu, Y. Jiang, Z. J. Wei, M. X. Gao, H. G. Pan and Q. D. Wang, *Phys. Chem. Chem. Phys.*, 2011, **13**, 314–321.
29 J. J. Hu, A. Pohl, S. M. Wang, J. Rothe and M. Fichtner, *J. Phys. Chem. C*, 2012, **116**, 20246–20253.
30 B. Li, Y. F. Liu, J. Gu, M. X. Gao and H. G. Pan, *Chem. Asian J.*, 2013, **8**, 374–384.
31 Y. F. Liu, J. J. Hu, Z. T. Xiong, G. T. Wu and P. Chen, *J. Mater. Res.2007*, **22**, 1339–1345.
32 J. H. Wang, T. Liu, G. T. Wu, W. Li, Y. F. Liu, C. M. Araujo, R. H. Scheicher, A. Blomqvist, R. Ahuja, Z. T. Xiong, P. Yang, M. X.

Gao, H. G. Pan and P. Chen, *Chem. Int. Ed.*, 2009, **48**, 5828–5832.
33 W. Luo, V. Stavila and L. E. Klebanoff, *Int. J. Hydrogen Energy*, 2012, **37**, 6646–6652.
34 Y. F. Liu, C. Li, B. Li, M. X. Gao and H. G. Pan, *J. Phys. Chem. C*, 2013, **117**, 866−875.
35 C. Liang, Y. F. Liu, M. X. Gao and H. G. Pan, *J. Mater. Chem. A*, 2013, **1**, 5031−5036.
36 C. Li, Y. F. Liu, Y. P. Pang, Y. J. Gu, M. X. Gao and H. G. Pan, *Dalton Trans*., 2014, **43**, 2369−2377.
37 C. Li, Y. F. Liu, Y. J. Gu, M. X. Gao and H. G. Pan, *Chem. Asian J*., 2013, **8**, 2136−2143.
38 T. Durojaiye, J. Hayes and A. Goudy, *J. Phys. Chem. C*, 2013, **117**, 6554−6560.
39 T. Durojaiye, J. Hayes and A. Goudy, *Int. J. Hydrogen Energy*, 2015, **40**, 2266−2273.
40 C. Li, Y. F. Liu, R. J. Ma, X. Zhang, Y. Li, M. X. Gao and H. G. Pan, *ACS Appl. Mater. Interfaces*, 2014, **6**, 17024−17033.
41 J. J. Hu, Z. T. Xiong, G. T. Wu, P. Chen, K. Murata and K. J. Sakata, *Power Sources*, 2006, **159**, 120−125.
42 J. J. Hu, Y. F. Liu, G. T. Wu, Z. T. Xiong and P. Chen, *J. Phys. Chem. C*, 2007, **111**, 18439–18443.
43 Y. L. Teng, T. Ichikawa, H. Miyaoka and Y. Kojima, *Chem. Comm.*, 2011, **47**, 12227−12229.
44 C. Liang, Y. F. Liu, K. Luo, B. Li, M. X. Gao, H. G. Pan, Q. D. Wang, *Chem. Eur. J.*, **2010**, 16, 693-702.
45 J. H. Wang, G. T. Wu, Y. S. Chua, J. P. Guo, Z. T. Xiong, Y. Zhang, M. X. Gao, H. G. Pan and P. Chen, *ChemSusChem*, 2011, **4**, 1622−1628.

Graphical contents entry:

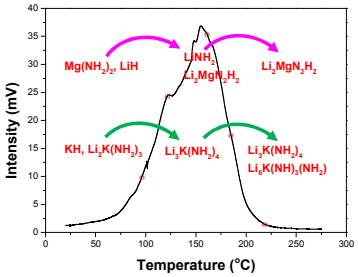

KH and $Li_2K(NH_2)_3$, formed *in situ* during ball milling, participate as reactants in the dehydrogenation reaction of the $Mg(NH_2)_2$-2LiH system.